Chemical Science

ROYAL SOCIETY OF CHEMISTRY

EDGE ARTICLE

View Article Online
View Journal | View Issue

Open Access Article. Published on 05 February 2024. Downloaded on 1/16/2026 7:56:25 PM.
This article is licensed under a Creative Commons Attribution-NonCommercial 3.0 Unported Licence.

Check for updates

Cite this: *Chem. Sci.*, 2024, **15**, 4068

All publication charges for this article have been paid for by the Royal Society of Chemistry

Supramolecular copolymerization of hydrophobic and hydrophilic monomers in liquid crystalline media†

Daiki Morishita,[a] Yoshimitsu Itoh,*[ab] Ko Furukawa,[c] Noriyoshi Arai,[d] Xu-Jie Zhang[a] and Takuzo Aida*[ae]

Received 25th November 2023
Accepted 4th February 2024

DOI: 10.1039/d3sc06341k

rsc.li/chemical-science

In the case of covalent polymers, immiscible polymers can be integrated by covalently linking them together, but such a strategy is not possible in supramolecular polymers. Here we report the supramolecular copolymerization of two porphyrin-based monomers, $^{C10}P_{2H}$ and $^{TEG}P_{Cu}$ with side chains bearing cyanobiphenyl (CB) groups at the ends of hydrophobic alkyl or hydrophilic tetraethylene glycol chains, respectively. These monomers undergo self-sorting supramolecular polymerization in highly diluted solutions ([monomer] = 3.4×10^{-9} mol% (2.0×10^{-8} mol L^{-1})) in nonpolar media due to the incompatibility of the side chains. Surprisingly, these monomers undergo supramolecular copolymerization under high concentration conditions ([monomer] = 7.7 mol%) in the medium of 4-cyano-4′-pentyloxybiphenyl (5OCB) to form a columnar liquid crystalline phase under thermodynamic conditions, where the individual columns are composed of supramolecular block copolymers. The combination of CB ends of both monomers and the 5OCB medium is essential for the two monomers to form an integrated structure in a condensed system without phase separation.

Introduction

Polymer mixtures may undergo macroscopic phase separation due to the small contribution of mixing entropy at high degrees of polymerization.[1,2] When mixing enthalpy is positive and large, as in mixing hydrophobic and hydrophilic polymers, immiscibility is further increased. Covalent linkage between the ends of such polymers to make a block copolymer prevents macroscopic phase separation, resulting in integrated structures such as microphase-separated structures.[3–6] In contrast to covalent polymers, the monomers in supramolecular polymers are connected noncovalently.[7–14] Therefore, we cannot force the two immiscible supramolecular polymers to form a block copolymer because the non-covalent connection between the two is energetically disfavored.[15,16] Currently, a guiding principle to mix two immiscible supramolecular polymers to form an integrated structure is missing.

In this study, we report that monomers $^{C10}\mathbf{P_{2H}}$ and $^{TEG}\mathbf{P_{Cu}}$ (Fig. 1a), which form hydrogen-bonded (H-bonded) supramolecular polymers and are not compatible with each other, can be copolymerized without macroscopic phase separation. This was achieved by employing nematic-forming 4-cyano-4′-pentyloxybiphenyl (5OCB) as a polymerization medium (Fig. 1b, middle). This liquid crystal (LC) system is designed based on our recent report on the formation of columnar LCs by supramolecular polymerization of disk-shaped monomers in a nematic LC medium composed of rod-shaped molecules.[17–19] The introduction of a mesogenic moiety at the termini of the disk-shaped monomer promotes the order-increasing mesophase transition from 1D to 2D to form a columnar LC ordering (Fig. 2). We have previously reported disk-shaped monomers having benzenetricarboxamide (BTA)[17,18] and porphyrin cores.[19] In the present work, we newly synthesized porphyrin-centered $^{TEG}\mathbf{P_{Cu}}$, bearing hydrophilic side chains. $^{C10}\mathbf{P_{2H}}$ and $^{TEG}\mathbf{P_{Cu}}$ are inherently immiscible due to the incompatible combination of the side chain units (conflicting pair). Thus, these two monomers do not mix homogeneously in bulk, and undergo self-sorting polymerization when mixed in a diluted solution of a nonpolar medium. Surprisingly, when these monomers are polymerized together in 5OCB, the entire material formed a columnar oblique (Col_{ob}) LC phase, where the individual column is composed of a block

[a]Department of Chemistry and Biotechnology, School of Engineering, The University of Tokyo, 7-3-1 Hongo, Bunkyo-ku, Tokyo 113-8656, Japan. E-mail: itoh@chembio.t.u-tokyo.ac.jp; aida@macro.t.u-tokyo.ac.jp

[b]Precursory Research for Embryonic Science and Technology (PRESTO), Japan Science and Technology Agency (JST), 4-1-8 Honcho, Kawaguchi, Saitama 332-0012, Japan

[c]Center for Coordination of Research Facilities, Institute for Research Administration, Niigata University, 8050 Ikarashi 2-no-cho, Nishi-ku, Niigata 950-2181, Japan

[d]Department of Mechanical Engineering, Keio University, 3-14-1 Hiyoshi, Kohoku-ku, Yokohama 223-8522, Japan

[e]Center for Emergent Matter Science (CEMS), RIKEN, 2-1 Hirosawa, Wako, Saitama 351-0198, Japan

† Electronic supplementary information (ESI) available. See DOI: https://doi.org/10.1039/d3sc06341k

© 2024 The Author(s). Published by the Royal Society of Chemistry

Open Access Article. Published on 05 February 2024. Downloaded on 1/16/2026 7:56:25 PM.
This article is licensed under a Creative Commons Attribution-NonCommercial 3.0 Unported Licence.

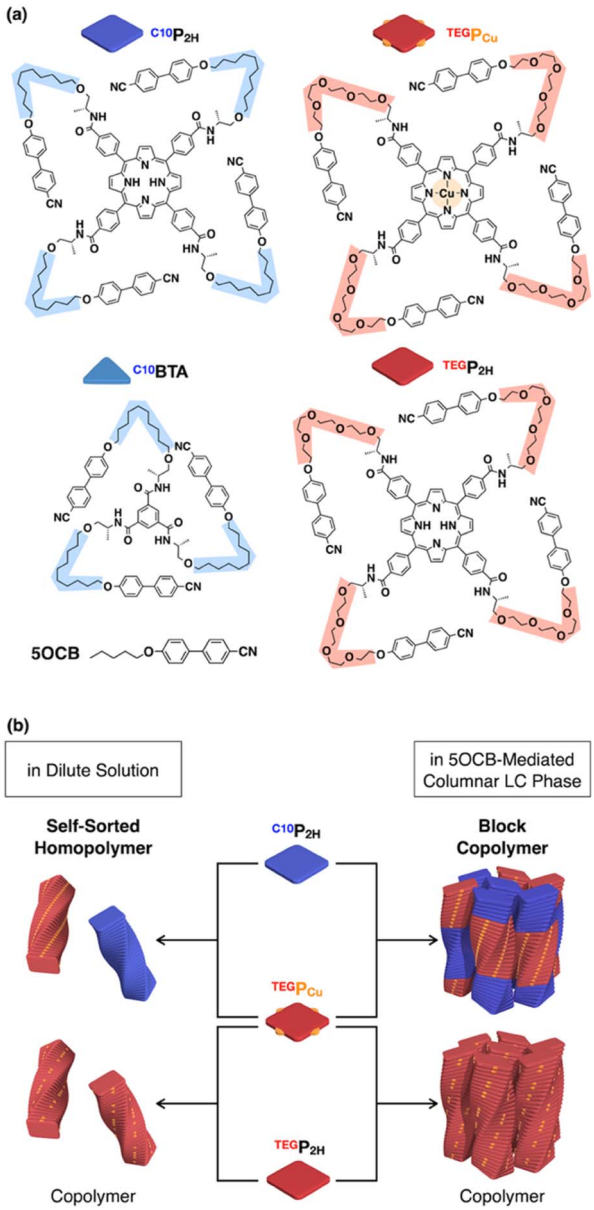

Fig. 1 (a) Molecular structures of H-bonding monomers $^{TEG}P_{2H}$, $^{TEG}P_{Cu}$, $^{C10}P_{2H}$, and ^{C10}BTA, and nematic LC molecule 5OCB. (b) Schematic representations of the supramolecular copolymerization of three different monomer pairs in 5OCB.

copolymer of the two monomers. The presence of 5OCB may suppress the macroscopic phase separation of two incompatible monomers and instead results in an integrated structure composed of supramolecular block copolymers. Considering that the supramolecular block copolymer is usually formed under kinetic conditions,[20–29] our system is one of the rare examples of the formation of a block sequence under thermodynamic conditions.[30–34] The present study may serve as a guiding principle for the control of the block sequence in supramolecular copolymers, that can lead to controlled microphase-separated structures as in conventional covalent copolymers.

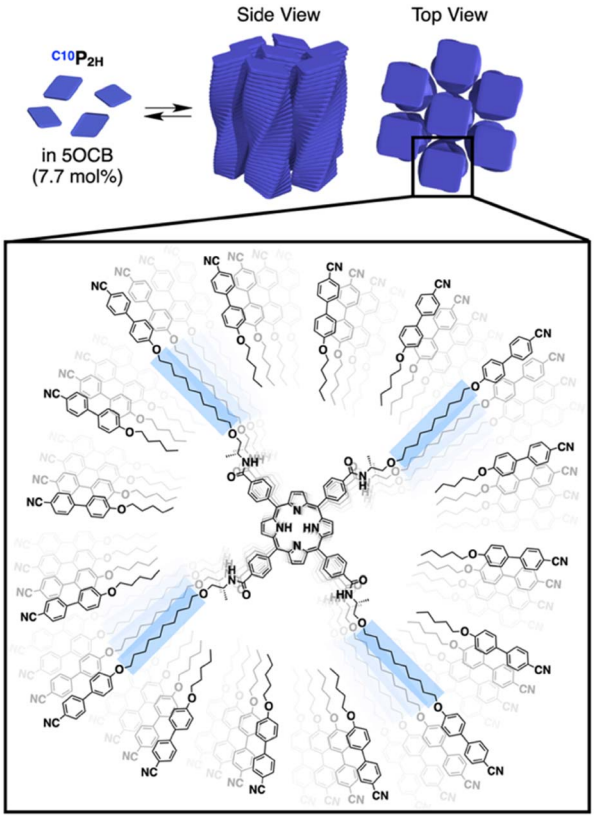

Fig. 2 Supramolecular polymerization of $^{C10}P_{2H}$ in a nematic-forming 5OCB medium, resulting in an order-increasing mesophase transition into a columnar LC structure.

Results and discussion

Monomer design and formation of columnar LCs

We have previously reported benzene-centered ^{C10}**BTA**[17] and porphyrin-centered ^{C10}**P**$_{2H}$,[19] both having oxycyanobiphenyl (OCB) terminated side chains appended with a chiral aliphatic chain (C10) that is connected to the core with an amide linkage. In this study, we newly synthesized two porphyrin-centered monomers, ^{TEG}**P**$_{Cu}$ and ^{TEG}**P**$_{2H}$ with chiral tetraethylene glycol (TEG) chains (Fig. 1a). The center of the monomer is either a free-base (**P**$_{2H}$) or copper(II) (**P**$_{Cu}$) porphyrin unit. It is known that the fluorescence of **P**$_{2H}$ is quenched by electron exchange with **P**$_{Cu}$ upon stacking (Dexter mechanism).[35–38] This allows us to evaluate whether the two monomers were copolymerized or not by using the fluorescence profile of the mixture.

Based on previous studies, ^{C10}**P**$_{2H}$ was mixed with 5OCB at a concentration of 7.7 mol% and heated up to 200 °C to obtain the isotropic melt. Upon cooling, this mixture was found to undergo phase transition at 110 °C to give a Col_{ob} LC phase by H-bonding mediated supramolecular polymerization, which was confirmed by differential scanning calorimetry (DSC), Fourier-transform infrared (FT-IR) spectroscopy, polarized optical microscopy (POM), and X-ray diffraction (XRD) measurements (Fig. 3a, f, S3a, S6a, S8a, and S13a, b†). The mixture exhibited a mesophase in a wide temperature range

Open Access Article. Published on 05 February 2024. Downloaded on 1/16/2026 7:56:25 PM.
This article is licensed under a Creative Commons Attribution-NonCommercial 3.0 Unported Licence.

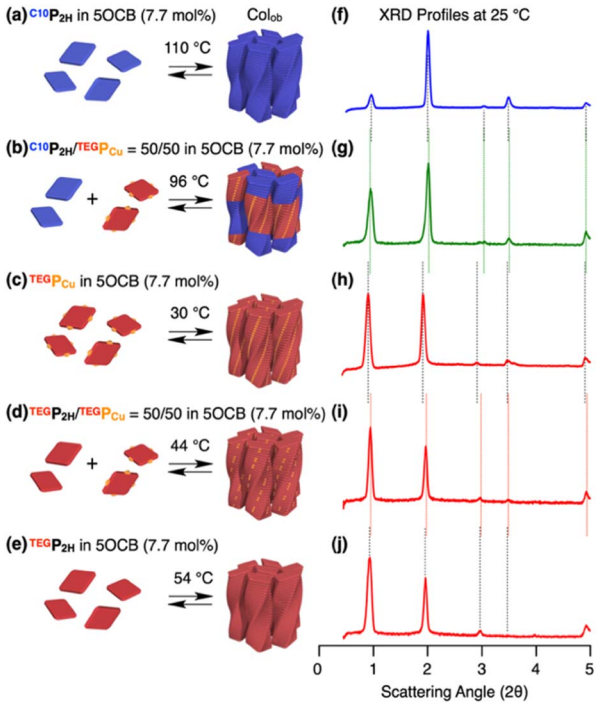

Fig. 3 (a–e) Schematic representations of the formation of columnar LCs and (f–j) XRD profiles at 25 °C of (a and f) $^{C10}P_{2H}$, (b and g) $^{C10}P_{2H}/^{TEG}P_{Cu}$ = 50/50, (c and h) $^{TEG}P_{Cu}$, (d and i) $^{TEG}P_{2H}/^{TEG}P_{Cu}$ = 50/50 and (e and i) $^{TEG}P_{2H}$ in 5OCB (7.7 mol%). The temperatures shown above the arrows in (a–e) are the LC phase transition temperatures obtained by DSC on cooling (5 °C min^{-1}).

between −20 and 110 °C including room temperature (a = 98.3 Å; b = 27.0 Å; γ = 70.7° at 25 °C) (Fig. S3a and S8a†). Electronic absorption spectra showed a sharp Soret band absorption at λ_{max} = 426 nm in the isotropic phase at 150 °C (Fig. 4a, gray). This indicates that the porphyrin monomers are not stacked in the isotropic phase. On the other hand, in the LC phase at 25 °C, Soret band absorption exhibited both red-shifted (434 nm) and blue-shifted (418 nm) bands (Fig. 4a, blue), which is typical for the formation of porphyrin J-aggregates.[39–43] Similarly, the newly synthesized $^{TEG}\mathbf{P_{Cu}}$ and $^{TEG}\mathbf{P_{2H}}$ with TEG chains were also confirmed to form a Col$_{ob}$ LC phase by supramolecular polymerization in 5OCB ([monomer] = 7.7 mol%) ($^{TEG}\mathbf{P_{Cu}}$: a = 99.6 Å; b = 25.7 Å; γ = 78.6°, $^{TEG}\mathbf{P_{2H}}$: a = 105.7 Å; b = 28.2 Å; γ = 71.0° at 25 °C, Fig. 3c, e, h, j, S3b, c, S6b, c, S8b, c and S13c–f†). Electronic absorption spectra showed Soret band absorption at λ_{max} = 423 nm for $^{TEG}\mathbf{P_{Cu}}$ and λ_{max} = 426 nm for $^{TEG}\mathbf{P_{2H}}$ in the isotropic phase at 150 °C (Fig. 4b and c, gray). In the LC phase at 25 °C, these bands exhibited both a red-shift (426 nm for $^{TEG}\mathbf{P_{Cu}}$ and 434 nm for $^{TEG}\mathbf{P_{2H}}$) and blue-shift (410 nm for $^{TEG}\mathbf{P_{Cu}}$ and 418 nm for $^{TEG}\mathbf{P_{2H}}$) (Fig. 4b and c, red). This is similar to that observed in the case of $^{C10}\mathbf{P_{2H}}$ (Fig. 4a) and suggests the formation of porphyrin J-aggregates for both $^{TEG}\mathbf{P_{Cu}}$ and $^{TEG}\mathbf{P_{2H}}$ in their Col LC phase.

Mixing of porphyrin monomers in columnar LC

We then performed a supramolecular copolymerization of a conflicting pair, $^{C10}\mathbf{P_{2H}}$ and $^{TEG}\mathbf{P_{Cu}}$, in 5OCB. The mixed LC of

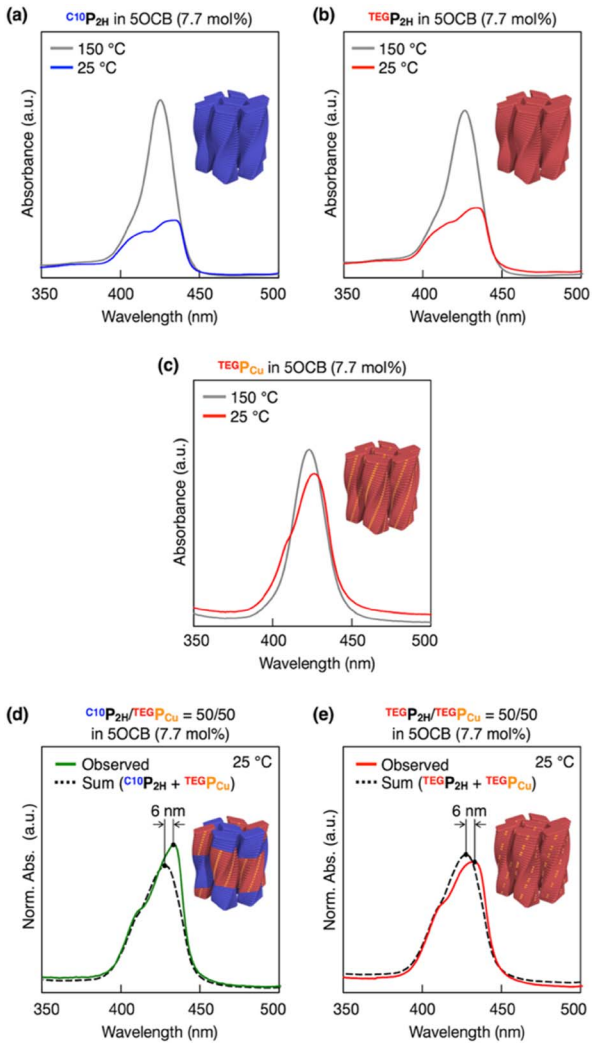

Fig. 4 Electronic absorption spectra of (a) $^{C10}P_{2H}$, (b) $^{TEG}P_{2H}$, (c) $^{TEG}P_{Cu}$, (d) $^{C10}P_{2H}/^{TEG}P_{Cu}$ = 50/50 and (e) $^{TEG}P_{2H}/^{TEG}P_{Cu}$ = 50/50 in 5OCB (7.7 mol%) at 25 °C. For (a) $^{C10}P_{2H}$, (b) $^{TEG}P_{2H}$, and (c) $^{TEG}P_{Cu}$ in 5OCB (7.7 mol%), electronic absorption spectra at 150 °C are also shown (gray). The summation of the electronic absorption spectra of $^{C10}P_{2H}$ in 5OCB (7.7 mol%) and $^{TEG}P_{Cu}$ in 5OCB (7.7 mol%) (d), and $^{TEG}P_{2H}$ in 5OCB (7.7 mol%) and $^{TEG}P_{Cu}$ in 5OCB (7.7 mol%) (e) is also shown (black dashed lines).

$^{C10}\mathbf{P_{2H}}/^{TEG}\mathbf{P_{Cu}}$ = 50/50 in 5OCB ([monomer] = 7.7 mol%) underwent a phase transition to the LC phase at 96 °C upon cooling (5 °C min^{-1}) from its isotropic melt at 200 °C. XRD measurement at 25 °C confirmed the formation of the Col$_{ob}$ LC phase (Fig. 3b, g S3d, S6d, S8d, and S14a, b†). Mixed LCs of $^{C10}\mathbf{P_{2H}}/^{TEG}\mathbf{P_{Cu}}$ = 75/25 and 25/75 in 5OCB ([monomer] = 7.7 mol%) also formed a Col$_{ob}$ LC phase (Fig. S4c, e, and S9c, e†). These results indicate that the two monomers can be mixed and form an integrated structure in 5OCB at arbitrary mixing ratios without macroscopic phase separation. It is noted that $^{C10}\mathbf{P_{2H}}$ and $^{TEG}\mathbf{P_{Cu}}$ have incompatible C10 and TEG side chains and undergo macroscopic phase separation in the bulk state (Fig. S27 and S28†) or in solution without 5OCB (Fig. S15 and S17†) (*vide infra*).[44] Therefore, it is surprising that these two porphyrin derivatives form an integrated structure in the LC

 © 2024 The Author(s). Published by the Royal Society of Chemistry

Open Access Article. Published on 05 February 2024. Downloaded on 1/16/2026 7:56:25 PM.
This article is licensed under a Creative Commons Attribution-NonCommercial 3.0 Unported Licence.

phase. The same mixing experiments were performed for the affinitive pair, $^{TEG}\mathbf{P_{2H}}$ and $^{TEG}\mathbf{P_{Cu}}$, both having common TEG side chains. The results indicate that they also form a single Col_{ob} LC phase without macroscopic phase separation (Fig. 3d, i, S3e, S6e, S8e, and S14c, d†).

Analysis by electronic absorption and fluorescence spectroscopy

To investigate how $^{C10}\mathbf{P_{2H}}$ and $^{TEG}\mathbf{P_{Cu}}$ are integrated in the LC phase, we performed electronic absorption and fluorescence spectroscopy of the mixed LC (Fig. 4 and 5). When the mixed LC of the conflicting pair ($^{C10}\mathbf{P_{2H}}/^{TEG}\mathbf{P_{Cu}}$ = 50/50 in 5OCB ([monomer] = 7.7 mol%)) was cooled from its isotropic melt at 150 °C to 25 °C at a ratio of 5 °C min^{-1}, it showed a Soret band absorption peak at 433 nm (Fig. 4d, green solid line). Compared to a simple summation of the absorption spectra of $^{C10}\mathbf{P_{2H}}$ in 5OCB ([monomer] = 7.7 mol%) and $^{TEG}\mathbf{P_{Cu}}$ in 5OCB ([monomer] = 7.7 mol%) (Fig. 4d, black dashed line), the absorption peak of the mixed LC exhibited a red-shift of 6 nm. Interestingly, the absorption spectral profile of the mixed LC of the affinitive pair ($^{TEG}\mathbf{P_{2H}}/^{TEG}\mathbf{P_{Cu}}$ = 50/50 in 5OCB ([monomer] = 7.7 mol%)) exhibited the same trend (Fig. 4e). This suggests that two monomers, no matter whether the monomer pair is conflicting ($^{C10}\mathbf{P_{2H}}/^{TEG}\mathbf{P_{Cu}}$) or affinitive ($^{TEG}\mathbf{P_{2H}}/^{TEG}\mathbf{P_{Cu}}$), are mixed in a single column in both mixed LCs. Then, the fluorescence spectra of LC samples were measured. LC samples containing only $^{C10}\mathbf{P_{2H}}$ or $^{TEG}\mathbf{P_{2H}}$ as a monomer showed characteristic fluorescence at λ_{em} = 650 nm and 715 nm upon excitation at λ_{ex} = 590 nm (Fig. S16†). When $^{TEG}\mathbf{P_{Cu}}$ was added to these LCs, the intensity of the fluorescence spectra decreased without a change in its shape (Fig. S16†), likely due to the electron exchange between $\mathbf{P_{2H}}$ and $\mathbf{P_{Cu}}$ which happens only when they are stacked.[35] Then, the fluorescence spectra of the mixed LCs at different %-mole fractions χ of $\mathbf{P_{Cu}}$ ($\chi = \mathbf{P_{Cu}}/(\mathbf{P_{Cu}} + \mathbf{P_{2H}})$ = 0, 10, 25, 50, 100%) were recorded (Fig. S16†), and the intensity of the spectral peak at λ_{em} = 650 nm relative to that at $\chi = 0$ (Fig. 5) was plotted. In both conflicting $^{C10}\mathbf{P_{2H}}/^{TEG}\mathbf{P_{Cu}}$ and affinitive $^{TEG}\mathbf{P_{2H}}/^{TEG}\mathbf{P_{Cu}}$ pairs, fluorescence quenching of $\mathbf{P_{2H}}$ was observed at $\chi = 10$ indicating the face-to-face stacking of $\mathbf{P_{2H}}$ and $\mathbf{P_{Cu}}$ (*i.e.* copolymerization) in either of the mixed LCs. This is consistent with the results obtained from the absorption spectra (Fig. 4). In addition, the degree of fluorescence quenching for conflicting $^{C10}\mathbf{P_{2H}}/^{TEG}\mathbf{P_{Cu}}$ LC is smaller than that for affinitive $^{TEG}\mathbf{P_{2H}}/^{TEG}\mathbf{P_{Cu}}$ LC. This trend was also observed in relative fluorescence lifetimes of the same mixed LCs (Fig. S18 and Table S1†). This may suggest that although $^{C10}\mathbf{P_{2H}}$ and $^{TEG}\mathbf{P_{Cu}}$ form a single columnar LC phase without macroscopic phase separation, the incompatibility of the side chains may favor homo-interaction over hetero-interaction at the microscopic level.

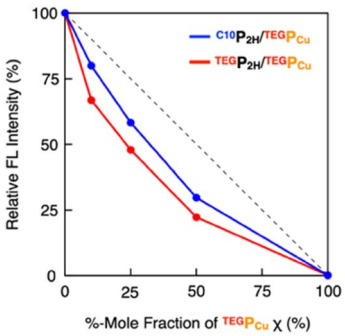

Fig. 5 Plots of relative fluorescence intensity (at λ_{em} = 650 nm and λ_{ex} = 590 nm) at different %-mole fractions χ of $^{TEG}P_{Cu}$ for the mixed LC of $^{C10}P_{2H}/^{TEG}P_{Cu}$ (blue) and $^{TEG}P_{2H}/^{TEG}P_{Cu}$ (red) in 5OCB (7.7 mol%).

In sharp contrast, the supramolecular polymerization of the mixed samples in diluted solution ([monomer] = 3.4 × 10^{-9} mol% (2.0 × 10^{-8} mol L^{-1})) in dodecane/chlorocyclohexane (54 : 46) was distinct from that in the LC state. In the case of the conflicting $^{C10}\mathbf{P_{2H}}/^{TEG}\mathbf{P_{Cu}}$ pair, the electronic absorption spectrum of the mixed solution matched the summation of the absorption spectra of the individual polymers (Fig. S15a, c, d†). This indicates that the conflicting $^{C10}\mathbf{P_{2H}}/^{TEG}\mathbf{P_{Cu}}$ pair underwent self-sorting polymerization in a diluted solution. On the other hand, the absorption peak of the mixed solution of the affinitive $^{TEG}\mathbf{P_{2H}}/^{TEG}\mathbf{P_{Cu}}$ pair exhibited a red-shift of 4 nm compared to a simple summation of the absorption spectrum of $^{TEG}\mathbf{P_{2H}}$ and $^{TEG}\mathbf{P_{Cu}}$ solutions (Fig. S15b, c, e†). This indicates that the affinitive $^{TEG}\mathbf{P_{2H}}/^{TEG}\mathbf{P_{Cu}}$ pair underwent copolymerization. These results were also supported by the fluorescence quenching experiment, where the fluorescence quenching was only obvious for the affinitive $^{TEG}\mathbf{P_{2H}}/^{TEG}\mathbf{P_{Cu}}$ pair (Fig. S17†). These results indicate that the copolymerization of $^{C10}\mathbf{P_{2H}}$ and $^{TEG}\mathbf{P_{Cu}}$ occurs only in a medium of 5OCB under highly concentrated conditions.

Analysis by electron spin resonance (ESR) spectroscopy

We investigated how the conflicting $^{C10}\mathbf{P_{2H}}/^{TEG}\mathbf{P_{Cu}}$ pair was mixed in a single column by ESR spectroscopy. In general, ESR spectra of Cu(II) change drastically when those spins interact with each other.[45–48] It is known that dispersed $\mathbf{P_{Cu}}$ gives a sharp spectrum with a narrow line width (Fig. 6a, simulated spectrum A).[45–47] On the other hand, when $\mathbf{P_{Cu}}$ are close to each other so that interactions between the Cu(II) spins due to orbital overlap take place, it is known to give a broad spectrum (Fig. 6a, simulated spectrum B).[46–48] In the case where one (or more) $\mathbf{P_{2H}}$ is intercalated between $\mathbf{P_{Cu}}$, the interaction between the Cu(II) spins is prohibited thus giving a sharp spectrum like spectrum A (Fig. 6a). We expected that this characteristic spectral feature could be used to evaluate the internal structure of an individual column, that is a copolymer composed of $^{C10}\mathbf{P_{2H}}$ and $^{TEG}\mathbf{P_{Cu}}$. Thus, we measured the ESR spectra of four LC samples, $^{C10}\mathbf{P_{2H}}/^{TEG}\mathbf{P_{Cu}}$ = 99/1, 90/10, 50/50, and 0/100 in 5OCB ([monomer] = 7.7 mol%).[44] Interestingly, we found that the ESR spectra of all four samples can be represented as either spectrum A or B, or their summation (Fig. 6b–e). For example, the mixed LC of $^{C10}\mathbf{P_{2H}}/^{TEG}\mathbf{P_{Cu}}$ = 99/1 in 5OCB ([monomer] = 7.7 mol%), forming a single Col_{ob} LC phase, gave a sharp ESR spectrum with a narrow line width identical to that of spectrum A (Fig. 6b). This indicates that $^{TEG}\mathbf{P_{Cu}}$ monomers, which are present in only 1% of the total monomers, are separated from each other. On the other hand, the Col_{ob} LC phase of the single-monomer LC of $^{TEG}\mathbf{P_{Cu}}$ in 5OCB ([monomer] = 7.7 mol%) gave an ESR spectrum that could be represented as a summation of

Open Access Article. Published on 05 February 2024. Downloaded on 1/16/2026 7:56:25 PM.
This article is licensed under a Creative Commons Attribution-NonCommercial 3.0 Unported Licence.

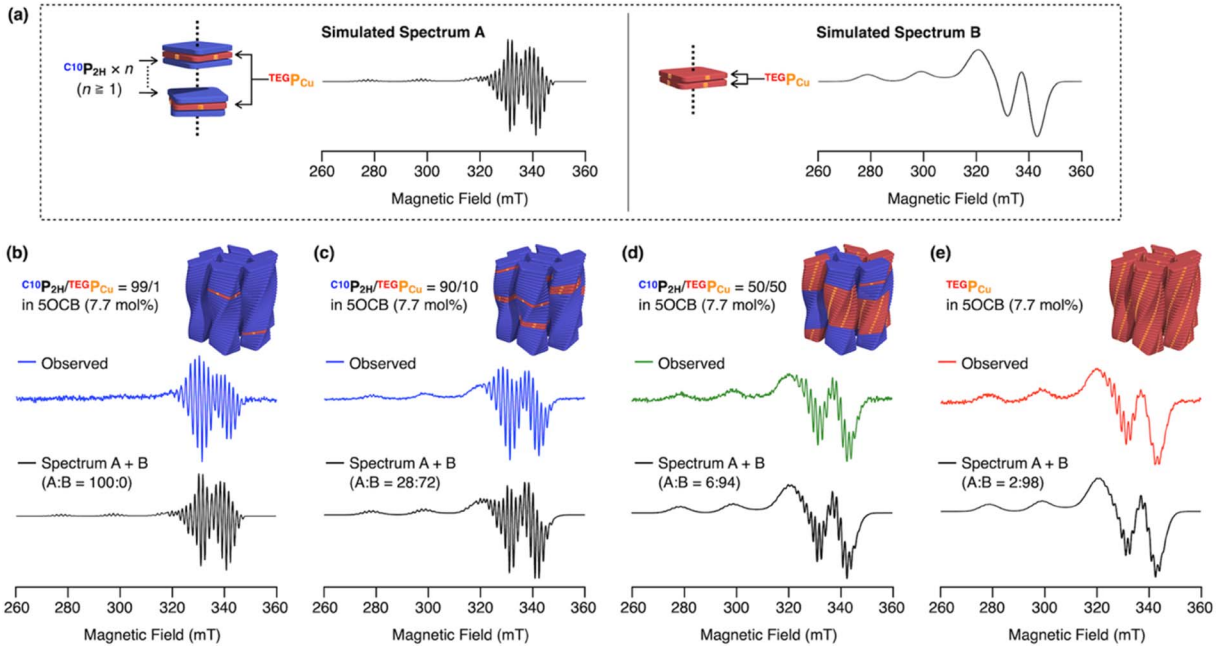

Fig. 6 (a) ESR spectra typical of P_{Cu} without Cu(II) spin–spin interactions (spectrum A) and with spin–spin interactions (spectrum B), generated by using the MATLAB® package of EasySpin®. (b–e) Obtained ESR spectra of (b) $^{C10}P_{2H}/^{TEG}P_{Cu}$ = 99/1, (c) $^{C10}P_{2H}/^{TEG}P_{Cu}$ = 90/10, (d) $^{C10}P_{2H}/^{TEG}P_{Cu}$ = 50/50 and (e) $^{TEG}P_{Cu}$ in 5OCB (7.7 mol%). The summation of spectrum A and spectrum B is also shown (black).

a broad spectrum B (98%) and a sharp spectrum A (2%) (Fig. 6e). This shows that the $^{TEG}\mathbf{P_{Cu}}$ monomers were mostly stacked with each other and only 2% formed a non-stacked disordered structure. When we performed ESR spectroscopy of the mixed LC of $^{C10}\mathbf{P_{2H}}/^{TEG}\mathbf{P_{Cu}}$ = 50/50 in 5OCB ([monomer] = 7.7 mol%), the spectrum could be represented as a summation of spectrum A (6%) and spectrum B (94%) (Fig. 6d). This result is surprising considering that an ESR spectrum of a statistically random co-stacking of $^{TEG}\mathbf{P_{Cu}}$ and $^{C10}\mathbf{P_{2H}}$ would be the sum of 25% A and 75% B. The experimental result indicates that as much as 94% of the total $^{TEG}\mathbf{P_{Cu}}$ monomers in the mixture are stacked with each other. The ESR spectrum of the mixed LC of $^{C10}\mathbf{P_{2H}}/^{TEG}\mathbf{P_{Cu}}$ = 90/10 in 5OCB ([monomer] = 7.7 mol%) was represented as a sum of 28% A and 72% B (Fig. 6c). Considering that a statistically random copolymer should be the sum of 81% A and 19% B, this result also showed that $^{TEG}\mathbf{P_{Cu}}$ prefers the homo-interaction. Together with the fluorescence spectral profiles, the $^{C10}\mathbf{P_{2H}}/^{TEG}\mathbf{P_{Cu}}$-based integrated Col_{ob} LCs are likely composed of supramolecular block copolymers of the two monomers.[44] In the previous examples, the formation of supramolecular block copolymers is governed by the balance between the association energies between the monomers (homo- and hetero-interactions).[30–34] In the present case, compatibilizing 5OCB seems to contribute to controlling this energy balance to realize a block sequence with the two monomers, which otherwise undergo self-sorting supramolecular polymerization.

Molecular simulation of the LC structures

The above results are also supported by the coarse-grained molecular simulations. First, the columnar LC structure was constructed using $^{C10}\mathbf{P_{2H}}$ and 5OCB (Fig. S23†), and equilibrated using constant-temperature simulation. The columnar LC structure turned out to be stable for more than 100 ns without structural collapse (Fig. S24†). When half of the $^{C10}\mathbf{P_{2H}}$ molecules in the model were randomly replaced with $^{TEG}\mathbf{P_{Cu}}$ and the same constant-temperature simulation was performed, the integrated columnar LC structure was stable as well (Fig. S25†). Finally, a simulation was performed in which all 5OCB molecules were changed to virtual solvent particles from the initial configuration of the columnar LC containing both $^{C10}\mathbf{P_{2H}}$ and $^{TEG}\mathbf{P_{Cu}}$. After 200 ns, the columnar structure collapsed and a single cluster composed of separated $^{C10}\mathbf{P_{2H}}$ and $^{TEG}\mathbf{P_{Cu}}$ was formed at equilibrium (Fig. S26†). These results are consistent with our experimental results that both monomers do not mix homogeneously in the bulk state[44] but can be integrated into a columnar structure in the presence of 5OCB.

Mixing of porphyrin monomers and BTA monomers in columnar LC

The above experiments showed that two porphyrin-centered monomers having incompatible side chains, $^{C10}\mathbf{P_{2H}}$ and $^{TEG}\mathbf{P_{Cu}}$ can be integrated in the presence of compatibilizing 5OCB. We then considered mixing $^{C10}\mathbf{P_{2H}}$ and $^{C10}\mathbf{BTA}$ (Fig. 1). Although both monomers have the same side chains, their different core sizes and number of amide groups make H-bonding-based copolymerization difficult. In such cases, is it possible for 5OCB to compatibilize $^{C10}\mathbf{P_{2H}}$ and $^{C10}\mathbf{BTA}$?. When $^{C10}\mathbf{BTA}$ was mixed in 5OCB at a concentration of 11 mol%, a single columnar hexagonal LC phase (a = 41.6 Å at 80 °C) was formed (Fig. 7c, f, S5e, S7b and S11b†). In the case of $^{C10}\mathbf{P_{2H}}$, it formed a Col_{ob} LC phase (a = 100.0 Å; b = 27.8 Å; γ = 71.6° at 80 °C) at 11 mol% concentration in

 © 2024 The Author(s). Published by the Royal Society of Chemistry

Open Access Article. Published on 05 February 2024. Downloaded on 1/16/2026 7:56:25 PM.
This article is licensed under a Creative Commons Attribution-NonCommercial 3.0 Unported Licence.

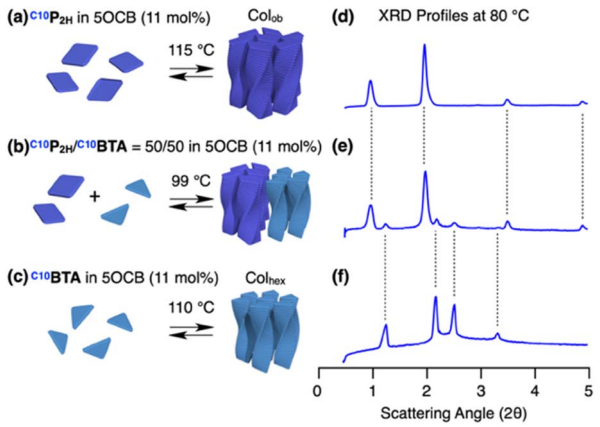

Fig. 7 (a–c) Schematic representations of the formation of columnar LC and (d–f) XRD profiles at 80 °C of (a and d) $^{C10}P_{2H}$, (b and e) $^{C10}P_{2H}/^{C10}BTA$ = 50/50 and (c and f) ^{C10}BTA in 5OCB (11 mol%). The temperatures shown above the arrows in (a–c) are the LC phase transition temperatures obtained by DSC on cooling (5 °C min^{-1}).

5OCB (Fig. 7a, d, S5a, S7a and S11a†). The mixed LC of $^{C10}\mathbf{P_{2H}}/^{C10}\mathbf{BTA}$ = 50/50 in 5OCB ([monomer] = 11 mol%) underwent a phase transition to a LC phase at 99 °C upon cooling (5 °C min^{-1}) from its isotropic melt at 200 °C (Fig. 7b and S5c†). The XRD profile obtained at 80 °C was represented as a summation of the diffraction patterns of the columnar LCs of $^{C10}\mathbf{P_{2H}}$ in 5OCB ([monomer] = 11 mol%) and $^{C10}\mathbf{BTA}$ in 5OCB ([monomer] = 11 mol%) (Fig. 7e). This indicates that both monomers formed their own columnar LC phases separately (Fig. 7d–f). In the POM images of the mixed LC, two different textures were observed, which were similar to that observed for the single monomer LC of $^{C10}\mathbf{P_{2H}}$ and $^{C10}\mathbf{BTA}$, indicating macroscopic phase separation (Fig. S7†). The samples with $^{C10}\mathbf{P_{2H}}/^{C10}\mathbf{BTA}$ = 25/75 and 75/25 also showed similar phase separation (Fig. S12†). These results suggest that 5OCB cannot compatibilize a pair of monomers having different preferences in H-bonding pattern and/or LC ordering.

Conclusions

In this study, we found that $^{C10}\mathbf{P_{2H}}$ and $^{TEG}\mathbf{P_{Cu}}$, which have mutually incompatible side chains, form an integrated structure consisting of supramolecular block copolymers in the columnar LC phase in the presence of 5OCB. The key for this achievement is the compatibilization by 5OCB, which forms a columnar structure together with supramolecular polymers, suppressing the macroscopic phase separation of both monomers. This strategy of mixing incompatible polymers by using a mediator is expected to lead to the realization of microphase-separated structures in supramolecular polymers.

Data availability

All data are available in the manuscript or in the ESI.†

Author contributions

D. M., Y. I. and T. A. designed the research. D. M. and X.-J. Z. prepared and characterized the materials. K. F. designed and conducted ESR measurements. N. A. carried out MD simulation. D. M. and Y. I. wrote the manuscript, with contributions from all authors.

Conflicts of interest

There are no conflicts to declare.

Acknowledgements

The synchrotron radiation experiments were performed on BL44B2 at the Super Photon Ring (SPring-8) with the approval of RIKEN (Proposal No. 20200031, 20210015, and 20220053). We acknowledge Dr K. Kato and Dr T. Hoshino from RIKEN SPring-8 center for their generous support for the synchrotron radiation experiments. This work was financially supported by a JSPS Grant-in-Aid for Scientific Research (S) (18H05260) on "Innovative Functional Materials based on Multi-Scale Interfacial Molecular Science" and Specially Promoted Research (23H05408) on "Solid-State Materials Science of Supramolecular Polymers and Their Applications" for T. A. Y. I. is grateful for a JSPS Grant-in-Aid for Young Scientist (A) (16H06035), Scientific Research (B) (21H01903) and the JST PRESTO grant JPMJPR21Q1. D. M. thanks the University Fellowship Founding Project for Innovation Creation in Science and Technology, "Fellowship for Integrated Materials Science and Career Development".

Notes and references

1 P. J. Flory, *J. Chem. Phys.*, 1941, **9**, 660.
2 M. L. Huggins, *J. Phys. Chem.*, 1942, **46**, 151–158.
3 C. M. Bates and F. S. Bates, *Macromolecules*, 2017, **50**, 3–22.
4 L. Leibler, *Macromolecules*, 1980, **13**, 1602–1617.
5 F. S. Bates and G. H. Fredrickson, *Annu. Rev. Phys. Chem.*, 1990, **41**, 525–557.
6 M. W. Matsen and F. S. Bates, *Macromolecules*, 1996, **29**, 1091–1098.
7 J. A. A. W. Elemans, A. E. Rowan and R. J. M. Nolte, *J. Mater. Chem.*, 2003, **13**, 2661–2670.
8 T. F. A. De Greef, M. M. J. Smulders, M. Wolffs, A. P. H. J. Schenning, R. P. Sijbesma and E. W. Meijer, *Chem. Rev.*, 2009, **109**, 5687–5754.
9 T. Aida, E. W. Meijer and S. I. Stupp, *Science*, 2012, **335**, 813–817.
10 K. Liu, Y. Kang, Z. Wang and X. Zhang, *Adv. Mater.*, 2013, **25**, 5530–5548.
11 E. Moulin, J. J. I. Armao and N. Giuseppone, *Acc. Chem. Res.*, 2019, **52**, 975–983.
12 M. Wehner and F. Würthner, *Nat. Rev. Chem*, 2020, **4**, 38–53.
13 T. Aida and E. w. Meijer, *Isr. J. Chem.*, 2020, **60**, 33–47.
14 P. K. Hashim, J. Bergueiro, E. W. Meijer and T. Aida, *Prog. Polym. Sci.*, 2020, **105**, 101250.

Open Access Article. Published on 05 February 2024. Downloaded on 1/16/2026 7:56:25 PM.
This article is licensed under a Creative Commons Attribution-NonCommercial 3.0 Unported Licence.

15 B. Adelizzi, N. J. Van Zee, L. N. J. de Windt, A. R. A. Palmans and E. W. Meijer, *J. Am. Chem. Soc.*, 2019, **141**, 6110–6121.
16 H. M. M. ten Eikelder, B. Adelizzi, A. R. A. Palmans and A. J. Markvoort, *J. Phys. Chem. B*, 2019, **123**, 6627–6642.
17 K. Yano, Y. Itoh, F. Araoka, G. Watanabe, T. Hikima and T. Aida, *Science*, 2019, **363**, 161–165.
18 K. Yano, T. Hanebuchi, X.-J. Zhang, Y. Itoh, Y. Uchida, T. Sato, K. Matsuura, F. Kagawa, F. Araoka and T. Aida, *J. Am. Chem. Soc.*, 2019, **141**, 10033–10038.
19 X.-J. Zhang, D. Morishita, T. Aoki, Y. Itoh, K. Yano, F. Araoka and T. Aida, *Chem.–Asian J.*, 2022, **17**, e202200223.
20 W. Zhang, W. Jin, T. Fukushima, A. Saeki, S. Seki and T. Aida, *Science*, 2011, **334**, 340–343.
21 Q. Wan, W.-P. To, X. Chang and C.-M. Che, *Chem*, 2020, **6**, 945–967.
22 W. Wagner, M. Wehner, V. Stepanenko and F. Würthner, *CCS Chem.*, 2019, **1**, 598–613.
23 W. Wagner, M. Wehner, V. Stepanenko and F. Würthner, *J. Am. Chem. Soc.*, 2019, **141**, 12044–12054.
24 A. Sarkar, R. Sasmal, C. Empereur-mot, D. Bochicchio, S. V. K. Kompella, K. Sharma, S. Dhiman, B. Sundaram, S. S. Agasti, G. M. Pavan and S. J. George, *J. Am. Chem. Soc.*, 2020, **142**, 7606–7617.
25 A. Sarkar, R. Sasmal, A. Das, S. S. Agasti and S. J. George, *Chem. Commun.*, 2021, **57**, 3937–3940.
26 A. Sarkar, R. Sasmal, A. Das, A. Venugopal, S. S. Agasti and S. J. George, *Angew. Chem., Int. Ed.*, 2021, **60**, 18209–18216.
27 S. H. Jung, D. Bochicchio, G. M. Pavan, M. Takeuchi and K. Sugiyasu, *J. Am. Chem. Soc.*, 2018, **140**, 10570–10577.
28 C. Jarrett-Wilkins, X. He, H. E. Symons, R. L. Harniman, C. F. J. Faul and I. Manners, *Chem.–Eur. J.*, 2018, **24**, 15556–15565.
29 D. Görl, X. Zhang, V. Stepanenko and F. Würthner, *Nat. Commun.*, 2015, **6**, 7009.
30 B. Adelizzi, A. Aloi, A. J. Markvoort, H. M. M. Ten Eikelder, I. K. Voets, A. R. A. Palmans and E. W. Meijer, *J. Am. Chem. Soc.*, 2018, **140**, 7168–7175.
31 A. Sarkar, T. Behera, R. Sasmal, R. Capelli, C. Empereur-mot, J. Mahato, S. S. Agasti, G. M. Pavan, A. Chowdhury and S. J. George, *J. Am. Chem. Soc.*, 2020, **142**, 11528–11539.
32 L. López-Gandul, A. Morón-Blanco, F. García and L. L. Sánchez, *Angew. Chem., Int. Ed.*, 2023, **62**, e202308749.
33 L. N. J. de Windt, Z. Fernández, M. Fernández-Míguez, F. Freire and A. R. A. Palmans, *Chem.–Eur. J.*, 2022, **28**, e202103691.
34 B. Adelizzi, P. Chidchob, N. Tanaka, B. A. G. Lamers, S. C. J. Meskers, S. Ogi, A. R. A. Palmans, S. Yamaguchi and E. W. Meijer, *J. Am. Chem. Soc.*, 2020, **142**, 16681–16689.
35 O. Ohno, Y. Ogasawara, M. Asano, Y. Kajii, Y. Kaizu, K. Obi and H. Kobayashi, *J. Phys. Chem.*, 1987, **91**, 4269–4273.
36 S. Prathapan, T. E. Johnson and J. S. Lindsey, *J. Am. Chem. Soc.*, 1993, **115**, 7519–7520.
37 M. S. Asano, K. Okamura, A. Jin-mon, S. Takahashi and Y. Kaizu, *Chem. Phys.*, 2013, **419**, 250–260.
38 G. A. Schick, I. C. Schreiman, R. W. Wagner, J. S. Lindsey and D. F. Bocian, *J. Am. Chem. Soc.*, 1989, **111**, 1344–1350.
39 J. H. van Esch, M. C. Feiters, A. M. Peters and R. J. M. Nolte, *J. Phys. Chem.*, 1994, **98**, 5541–5551.
40 R. van der Weegen, A. J. P. Teunissen and E. W. Meijer, *Chem.–Eur. J.*, 2017, **23**, 3773–3783.
41 N. Sasaki, M. F. J. Mabesoone, J. Kikkawa, T. Fukui, N. Shioya, T. Shimoaka, T. Hasegawa, H. Takagi, R. Haruki, N. Shimizu, S. Adachi, E. W. Meijer, M. Takeuchi and K. Sugiyasu, *Nat. Commun.*, 2020, **11**, 3578.
42 T. Yamaguchi, T. Kimura, H. Matsuda and T. Aida, *Angew. Chem., Int. Ed.*, 2004, **43**, 6350–6355.
43 S. Okada and H. Segawa, *J. Am. Chem. Soc.*, 2003, **125**, 2792–2796.
44 See ESI†
45 K. Tanaka, A. Tengeiji, T. Kato, N. Toyama and M. Shionoya, *Science*, 2003, **299**, 1212–1213.
46 S. Richert, I. Kuprov, M. D. Peeks, E. A. Suturina, J. Cremers, H. L. Anderson and C. R. Timmel, *Phys. Chem. Chem. Phys.*, 2017, **19**, 16057–16061.
47 N. Toyama, M. Asano-Someda and Y. Kaizu, *Mol. Phys.*, 2003, **101**, 733–742.
48 F. Hajjaj, K. Tashiro, H. Nikawa, N. Mizorogi, T. Akasaka, S. Nagase, K. Furukawa, T. Kato and T. Aida, *J. Am. Chem. Soc.*, 2011, **133**, 9290–9292.

 © 2024 The Author(s). Published by the Royal Society of Chemistry